

The Sunspot Cycle and Solar Magnetic Fields. I The Mechanism as Inferred from Observation

Ronald G. Giovanelli

Kitt Peak National Observatory*,
P.O. Box 26732, Tucson, AZ 85726, U.S.A.

Abstract

Observations of solar magnetic and velocity fields can be used to derive the course of events involved in the solar cycle. These differ in three important respects from those of conventional dynamo theories: (i) *Polar field reversal*. Following the outbreak of a new cycle, magnetic flux released by sunspots diffuses initially by Leighton's random-walk process, but this is soon dominated by the observed poleward flow of about 20 m s^{-1} which carries flux to polar regions in about 12 months. Since follower spots lie about 2° higher in latitude than leaders, follower flux arrives in polar regions some two weeks ahead of leader flux, providing a net inflow of follower polarity there until sunspot maximum, reversing the polar field from the previous sunspot cycle and building it up to a maximum. After sunspot maximum, the flux arriving in polar regions is predominantly of follower polarity until or unless spots occur at latitudes so low that flux can diffuse towards and across the equator, predominantly from the lower latitude leader; the effect is doubled by a complementary migration from the opposite hemisphere. This prevents the change in polar flux over the cycle from dropping to zero, and leaves the polarity there reversed at the end of the cycle. (ii) *The sunspot cycle*. A slow, deeper counterflow, essential for continuity, carries flux strands down in the polar zones and then equatorwards. The concentration of strands is increased continually by differential rotation, and they are dragged continually into contact. Reconnection occurs rapidly except between tubes that are inclined at very small angles. This results in the formation of ropes of flux strands twisted very gently. At some stage they are large enough to float, forming sunspots. The mean sunspot latitude decreases continuously as the flux is carried equatorwards, dying out as the flux ropes become exhausted. The whole process repeats, once again reversing the polar and spot group magnetic fields. Hale's polarity laws follow immediately, and Spörer's law requires only minor adjustments to the predicted velocity of the deep equatorward counterflow. The estimated velocity of this flow is compatible with the observed sunspot and magnetic cycles of 11 and 22 years. (iii) *The torsional oscillation*. Shear by differential rotation increases the concentration of flux strands; the reaction to strongly sheared flux strands is a tendency to reduce differential rotation. This results in cyclic variations of differential rotation, the phase with respect to sunspot formation being in good agreement with the torsional oscillation observations of Howard and LaBonte (1981) at all latitudes up to $50-55^\circ$.

1. Introduction

The modern theory of sunspots and the sunspot cycle started with Babcock's (1961) proposition that the cycle results from the action of the Sun's differential rotation in winding a general magnetic field. From this came his explanation of Spörer's law (see e.g. Spörer 1894) describing the variation of mean sunspot latitude during the

* Operated by the Association of Universities for Research in Astronomy, Inc., under contract with the National Science Foundation.

cycle, providing convincing evidence that, in some way or other, differential rotation is an essential ingredient of cycle theory. Leighton (1964) devised a neat mechanism whereby magnetic flux is transported over the Sun's surface, arguing that this would lead ultimately to reversal of the meridional component of the field and therefore to the full 22-year magnetic cycle. Since that time there has been intense activity in other attempts to explain the cycle, or to describe various aspects of it in greater detail, with special emphasis on dynamo and to a lesser extent primordial-field theories [for a survey see Cowling (1981)].

While based on observation, the Babcock–Leighton theory breaks down by comparison with observation in at least two respects which were unknown at the time it was developed:

- (i) Sunspots occur only at latitudes below 30–35° whereas, in Babcock's theory, field amplification and spot production should maximize at 45° and continue equally to low and high latitudes.
- (ii) Surface fields are always in the kilogauss range (Stenflo 1976) and never ~ 1 G as required by Babcock (who adopted 5 G) at the beginning of winding ($1 \text{ G} \equiv 10^{-4} \text{ T}$).

In addition, the discovery by Howard and LaBonte (1980) of torsional oscillations drifting from polar regions to low latitudes in about 22 years clearly demands a theory in which they can be incorporated.

The detailed discussion given here and in the companion paper (Giovanelli 1985; referred to as Part II, see present issue p. 1067) is based as closely as possible on observation, and covers the main phenomena of the cycle. In summary, flux released from sunspots in equal quantities of opposite polarities is dispersed by Leighton's random-walk mechanism, but this is dominated by the observed poleward flow of gas at speeds of $\sim 20 \text{ m s}^{-1}$ at latitudes from 10–70° [see Howard (1974); Duvall (1979); Howard and LaBonte (1980); J. M. Beckers (personal communication) gives higher velocities still]. The transport of flux to polar latitudes takes some 12 months. Rapid connection occurs in regions where flux tubes of opposite polarities are dragged into contact, leaving U-shaped strands which float ultimately out of the Sun, so reducing greatly the total absolute flux at the surface. In addition, the fully subsurface loops left after reconnection and the remaining strands passing through the surface are carried towards the poles by the poleward flow. The transient flux has a slight excess of follower polarity (the opposite from the polar fields at the beginning of the cycle) up to sunspot maximum, because of the phase lag due to the leader spot being closer to the equator; therefore, it reduces or reverses the polarity of the polar field. Later in the cycle, when spot groups are present at low latitudes, flux can diffuse across the equator to be swept towards the opposite pole. More leader than follower flux is involved in this because of the tilt of the spot-group axes. An equal quantity of flux of opposite polarity diffuses into the first hemisphere from the other, doubling the effect. Thus, there is an overall imbalance in the net flux of follower polarity carried to a polar region during the cycle, and the field there remains reversed at the end of each cycle.

The poleward flow must be balanced by a slow counterflow deeper in the convection zone, and this carries flux equatorwards. In the process, the flux is wound into an almost toroidal form by differential rotation. Thus, flux strands are brought closer and closer together and can be dragged into contact. Reconnection is rapid except

when the angle of contact between tubes is very small; flux ropes are then built up from flux fibres twisted very gently around one another. Although they predominate greatly in number, the fully subsurface continuous loops contribute nothing to the net flux in these ropes, for they carry equal fluxes of opposite signs and are annihilated ultimately in the reconnection processes. If large enough, a portion of a rope floats upwards to form sunspots. The equatorward drift ensures that this will occur first at some moderate latitude, after which the mean latitude of sunspot formation drifts towards the equator. The outbreak of new cycle spots brings us back to the starting point, except that all polarities are reversed. A full cycle in which polarities become the same as initially requires a second sunspot cycle, the length of the full cycle being approximately that required for the equatorward counterflow to go from polar regions to near the equator, i.e. ~ 20 yr.

The mean concentration of flux tubes increases in the convection zone because of shearing by differential rotation. Correspondingly, a large density of sheared flux tubes reacts back so as to reduce differential rotation. The net result is a torsional oscillation drifting from polar regions towards the equator, the maximum increase in the rate of rotation at a given latitude being expected about two years before maximum sunspot activity at that latitude. Below about 55° , the theory of the phase of the oscillation is in close agreement with the Howard and LaBonte (1980) observations. In Part II, the amplitude is also shown to be compatible with these observations.

The properties of the convection zone are not known in sufficient detail for a complete theory to be given at this stage. However, an approximate theory backed by surface observations enables the main features of the cycle to be understood. The present paper discusses what can be discovered without considering quantitatively the interactions between flux tubes and convective motions; these are described in Part II.

The numerical values so derived, being based on an approximate analysis, may change appreciably when an exact theory is developed. Values obtained so far have been fitted at each stage to suit the observations. This process has been repeated several times. It is probable that, as a consequence, significant errors are present in the physical quantities, which have been pulled into agreement at each stage; however, the physical principles, in which we are primarily interested here, remain unaffected.

2. Surface Fields during the Cycle and Related Processes

Sunspot formation is a cyclic or quasi-cyclic phenomenon, and the initial conditions for a given cycle are the terminal conditions of the preceding cycle. At sunspot minimum, the Sun is covered by magnetic elements of effectively random polarities, except in the polar regions, which are unipolar. The regions of mixed polarity have mean absolute fluxes (i.e. fluxes irrespective of sign) between about 3 and 10 G when averaged over large areas. As many authors have shown, the photospheric field is restricted to very small elements where B is typically 1000–2000 G.

As the cycle develops, the release of flux from sunspots is accompanied by the development of regions described as unipolar, though a small amount of flux of the opposite polarity is usually present within. Let us consider the details of this process.

Except possibly at sunspot minimum, Piddington's (1976*a*, Section 3) flux tree consisting of a rope frayed into hundreds or thousands of flux strands appears to

provide a fairly good description of the field configuration not too far below the surface in both unipolar regions and those of mixed polarity. At some stage, surface fields will be or will have been connected to fields somewhat stronger and narrower deep in the convection zone. It is well known that isolated flux strands are long lived provided that they are twisted (see e.g. Piddington 1975, 1976*b*, 1981; Giovanelli 1977), and there is a substantial body of evidence for twisting (Piddington 1976*b*, 1979). But flux strands are far from isolated and will interact if dragged into contact, which can happen wherever there are non-uniform gas motions, such as throughout the convection zone.

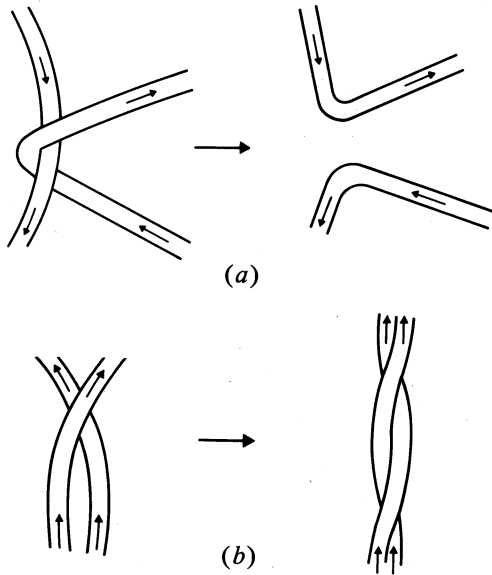


Fig. 1. (a) The result of the rapid subsurface reconnection of flux strands of opposite vertical polarities is a U-shaped upper strand, which can float out of the Sun, and a lower strand completely submerged. Reconnection occurs frequently, whenever flux strands are dragged into contact by differential gas motions. (b) Deep in the convection zone, tubes of force dragged or twisted into contact at very small angles can reconnect only very slowly. Thus, they build up ropes in which individual flux tubes may spiral in either sense.

Consider two flux tubes originating in flux ropes of opposite polarities, which intersect the surface and are being transported polewards. It will be common for gas motions to *drag* such tubes into contact (see Fig. 1*a*). Reconnection will occur when the separation between the tubes is small enough. Provided the tubes continue to be *dragged* together, reconnection continues until complete. Although this mechanism differs from that put forward by Petschek (1964), the rate can be no slower, about $0.01 V_A$ to $0.1 V_A$, where V_A is the Alfvén velocity (Priest and Soward 1976). If the tubes have identical fluxes, a U-shaped strand is produced with both ends passing out through the surface, together with a completely submerged loop connected on both sides back to the original flux rope. The U-shaped loop will be distorted by gas

motions. Fully submerged continuous loops may be cut off from it, or the U-shaped loop may reconnect with other flux tubes, but ultimately it will float up and escape. This must be a fairly rapid sequence. It is the only procedure whereby the absolute surface flux is reduced, and observation shows that the absolute flux present at any one time is but a small fraction of that liberated from sunspots. In practice, the original reconnecting flux tubes are unlikely to be of identical fluxes, and a portion of a surface flux tube will remain connected to the submerged loop. This residue cannot float away, but may possibly be the origin of the 'pepper and salt' fields (Livingston and Harvey 1975; Harvey 1977).

The fully submerged loop also undergoes distortion and reconnection as it is drawn polewards. Further loops are cut off either from itself or as a result of interaction with other tubes of force. In some cases these interactions may result in tubes passing out through the surface once more, as in the beginning. For most purposes we can disregard continuous submerged loops (such as those shown in Fig. 3 in Section 6), but they have a significant effect on the amplitude of the torsional oscillation (see Part II). Only a small but important minority of strands will avoid the reconnection process.

The situation described exists at almost any stage in the cycle. Even at sunspot minimum there is no meridional field but a large number of flux strands of at least kG strength.

3. Poleward Flow

Various fields of motion now act on the subsurface and residual surface strands, one being turbulent convection, a second being differential rotation. There is a third major field of gas motion, the systematic poleward flow discovered by Duvall (1979) as a result of sensitive measurements of Doppler shifts. In both hemispheres, there is a poleward drift of the order of 20 m s^{-1} . The accuracy of measurement is not great, but the order of magnitude is the same from 10° to 50° in latitude. This is much greater than the cyclic variations in meridional sunspot motion reported by Tuominen (1941, 1976) and Richardson and Schwarzschild (1953), which can be ignored by comparison. While these measurements were made at sunspot minimum, similar results have been obtained (T. L. Duvall, personal communication) through the recent solar maximum, so that the phenomenon appears to be independent of the phase of the cycle. Clearly the flow is zero at the equator and poles. At 20 m s^{-1} , the surface motion moves gases through 40° in latitude in about one year.

A meridional flow was required by Babcock (1961) to account for the migration of bipolar magnetic regions in latitude, except that he suggested that it was towards the equator in low latitudes and towards the poles in moderate latitudes. Howard (1974) reported flux migration polewards at about 20 m s^{-1} between latitudes of 40° and 70° . More recently LaBonte and Howard (1982) concluded that the poleward velocity of flux was $15\text{--}20 \text{ m s}^{-1}$ throughout the cycle. J. M. Beckers (personal communication) has also observed poleward motion of gases yielding Doppler shifts of up to 40 m s^{-1} . The best summary at present is that the flow is at a fairly uniform rate ($\sim 20 \text{ m s}^{-1}$) from about 10° to 70° in latitude, tapering off to zero at the poles and equator. For continuity, there must be a deeper counterflow forming a meridional circulation extending from about 70° to 10° in latitude. The mean velocity of the counterflow depends on the thicknesses of the poleward and equatorward flows.

The variation in depth ZP of the poleward flow can be incorporated into the continuity equation

$$\int_{ZP}^0 R \cos \phi \rho V_p dz = Q, \tag{1}$$

where R is the radius, ϕ is the latitude, ρ and V_p are the density and poleward velocity at depth z (positive outward), and Q is a circulation constant. To an adequate approximation (1) may be replaced by

$$R_p \bar{V}_p \cos \phi (\rho H_p)_{ZP} = Q, \tag{2}$$

where R_p is a mean radius, \bar{V}_p the average value of V_p with depth, and H_p the density scale height. As at the surface we assume that \bar{V}_p is uniform from 10° to 70° . Given ZP at any latitude in this range, the depth can then be found at any other latitude using data from Spruit's (1974) model. If ZP is given at 10° , its approximate values at other latitudes are as listed in Table 1. The depth increases towards the poles. If we choose ZP too deep at 10° latitude (e.g. 155 Mm; 1 Mm $\equiv 10^6$ m), then the depth exceeds that of the convection zone at high latitudes.

Table 1. Depth of the poleward flow for constant \bar{V}_p and three choices of the depth ZP at latitude 10°

Latitude	10°	20°	30°	40°	50°	60°	70°
ZP (10^5 km)	0.622	0.635	0.655	0.686	0.732	0.800	0.915
	0.994	1.00	1.03	1.08	1.15	1.25	1.42
	1.55	1.58	1.63	1.71	1.83	2.00	—

Properties of the counterflow can be estimated similarly. This must lie entirely within the convection zone (a formal proof is given in Part II) and, as a corollary, the tubes of force must also be confined to the convection zone.

It then follows, from continuity, that the relation equivalent to (1) is

$$\int_{ZE}^{ZP} R \cos \phi \rho V_e dz = Q \tag{3}$$

in the equatorward flow, where V_e is the equatorward velocity assumed variable with latitude and ZE is the depth to the base of the flow. The equation can be approximated by

$$R_e \bar{V}_e \cos \phi (\rho_{ZE} - \rho_{ZP}) H_{ZE} = Q, \tag{4}$$

where H_{ZE} and ρ_{ZE} are the density scale height and density at the base of the equatorward flow, ρ_{ZP} is the density at the base of the poleward flow, and R_e, \bar{V}_e are appropriate means of R, V_e with depth. The mean velocity of the equatorward flow V^* , when projected onto the solar surface, is

$$V^* = \frac{R_\odot \bar{V}_e}{R_e} = \frac{R_\odot R_p}{R_e^2} \frac{(\rho H_p)_{ZP}}{(\rho_{ZE} - \rho_{ZP}) H_{ZE}} \bar{V}_p. \tag{5}$$

If we take the base of the equatorward flow to be at the base of the convection zone, Spruit's (1974) model and Table 1 provide the data needed for calculating V^* . For \bar{V}_p we use 20 m s^{-1} , the surface value adopted for $10^\circ < \phi < 70^\circ$. The results are given in Table 2. As explained above, a depth of 155 Mm at $\phi = 10^\circ$ requires that at high latitudes the base of the poleward flow be deeper than the convection zone, which is invalid. It will appear in Section 6*d* that the base of the poleward flow ZP is probably in the range of the two top rows of Tables 1 and 2. The equatorward flow velocity decreases continuously as the latitude decreases.

If V_p and hence \bar{V}_p vary with latitude, the depth to the base of the equatorward flow will also vary. This point is scarcely fundamental to the analysis, and needs no further discussion here.

Table 2. Predicted velocities (in m s^{-1}) in the equatorward flow
 \bar{V}_p is assumed to be 20 m s^{-1}

ZP (10^5 km) at $\phi = 10^\circ$	$\phi =$	10°	20°	30°	40°	50°	60°	70°
0.622	$V^* =$	1.27	1.34	1.46	1.66	2.00	2.63	4.01
0.994		5.3	5.6	6.2	7.1	8.8	12.4	21.5
1.55		35	38	47	65	128	—	—

4. Transport of Flux across the Sun's Surface

The three fields of motion operate on the flux strands. Turbulent convection moves the strands about but, even deep in the convection zone, leaves the statistical properties of individual strands largely unchanged. Differential rotation causes a systematic realignment of flux strands away from the north-south direction. The surface meridional flow moves the whole system polewards. Combined with the other fields of motions, this results in the well-known inclination of unipolar regions eastwards towards higher latitudes.

In more detail, when flux is dispersed from sunspots by the unravelling of flux strands, it is carried by surface motions towards supergranule boundaries, near which most of the flux resides. Conventionally, these break down after about a day, the flux strands being dispersed by a random-walk process. Leighton (1964) described the transport of flux resulting from this combined with differential rotation. For flux released from unipolar concentrations of opposite polarities, he assumed that the fields add algebraically wherever the separate distributions overlap. The resulting isogauss maps appear decidedly similar to the unipolar regions that trail eastward and polewards from active regions. However, in this model diffusion occurs equally equatorwards, and this is observed only to a very modest extent as indicated, for example, by the arrival of unipolar regions in equatorial zones relatively late in the cycle (see e.g. Giovanelli 1982).

The poleward drift of the flux tubes poses an interesting problem. It is scarcely possible for gas velocities as low as 20 m s^{-1} to be able to transport flux tubes without the intervention of some other process. This process is the redistribution of tubes following the breakdown of supergranules at intervals of about a day. Flux released from a point then diffuses on average over a circle of radius $(2r/\pi)n_w^{1/2}$ in n_w days, r being the radius of a supergranule. For $r = 15 \text{ Mm}$, this amounts to about 90 Mm,

or 12° , in 90 days. In this time flux is carried polewards through 13° . Thus the main drift is polewards, with very little towards the equator except in the first few weeks after release, or very late in the cycle when the sunspots themselves lie so close to the equator that the poleward meridional velocity is small. Similar processes operate, on their appropriate scales, in the descending part of the counterflow near polar regions, stretching and carrying parts of tubes deep into the convection zone. These processes are examined in greater detail in Part II.

After sunspot generation has ceased at solar minimum, mixed-polarity regions cover almost the whole Sun. At this time, the poles are unipolar and of opposite polarities.

5. Reversal of Polarities in Polar Regions

Brunner's (1930) measurements of the tilts of spot-group axes from an east-west line showed an increase with latitude to a tilt of 19° in the latitude range $30\text{--}34^\circ$. Most of the flux released during a cycle is contained in the larger groups, where the separation of the spots commonly exceeds 10° in longitude. With the conservative choice of 10° , the follower spot is then further from the equator than the leader by over 3° for latitudes $30\text{--}34^\circ$ and about 2° for latitudes $20\text{--}29^\circ$. Thus, until sunspot maximum, flux is carried to polar regions earlier from follower than leader by the time taken for the poleward flow to travel typically 2° in latitude, about 14 days at 20 ms^{-1} . However, leader flux is released more slowly than follower, so that the 14-day lag is a lower limit. With a conservative 3-day difference in flux release, the typical lag is 17 days. Later in the cycle, the average lag decreases.

We now consider the flux released from sunspots during a single cycle. From minimum to maximum takes about 3 years, during which there is a phase advance of follower flux over leader. If in a given hemisphere the fluxes of each type liberated per unit time are equal to $\mathcal{F}(t)$, the difference in rate of arrival of follower and leader flux in polar regions after transit times T_t and $T_t + \Delta T_t$ respectively is

$$\mathcal{F}(t - T_t) - \mathcal{F}(t - T_t - \Delta T_t) \quad \text{or} \quad \{d\mathcal{F}(t - T_t)/dt\} \Delta T_t,$$

where $\Delta T_t \sim 17$ days (see Figs 2*a* and 2*b*). Thus the net flux which has arrived by time t is

$$\int_0^t \{d\mathcal{F}(t - T_t)/dt\} \Delta T_t dt = \mathcal{F}(t - T_t) \Delta T_t,$$

which mimics the curve of flux release.

The total flux of either polarity released during the cycle is $\int_0^{T_c} \mathcal{F}(t) dt$, where T_c is the length of the cycle. The ratio of the net flux to the total of either polarity released during the cycle is

$$\mathcal{F}(t - T_t) \Delta T_t / \int_0^{T_c} \mathcal{F}(t) dt.$$

At time ΔT_t after solar maximum, the ratio is of the order $\mathcal{F}_{\max} \Delta T_t / 0.5 \mathcal{F}_{\max} T_c$, or about 0.008 if $T_c = 11.3$ yr and $\Delta T_t = 17$ days.

In the later part of the cycle, spots appear close to the equator where the poleward flow becomes very small. The leader being closer to the equator than the follower,

supergranule motions transport more leader flux than follower across the equator into the other hemisphere, where they migrate to the opposite pole. As a consequence, the net flow of leader flux to the pole is reduced, and there is a net change in polar flux after the end of the cycle (see Figs 2c and 2d).

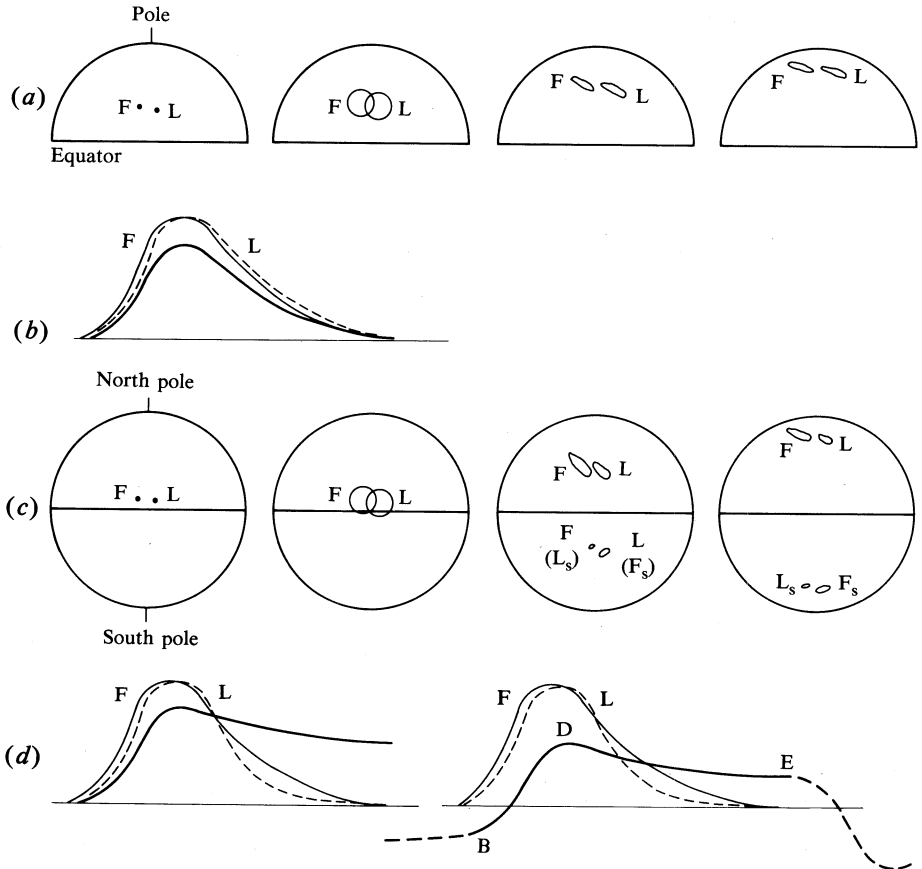


Fig. 2. (a) Migration of follower F and leader L flux towards poles without allowance for any diffusion of net L flux towards and across the equator later in the cycle. (b) Rates of arrival of F and L flux with zero flux cancellation during transit. The lower solid curve shows the net flux (not to scale). (c) Later in the cycle some flux from low latitude spots migrates into the opposite hemisphere (L_s and F_s), more from leader than follower. (d) The resulting polar flux, where the flux of follower polarity remains at E at transit time T_t after the end of the sunspot cycle, B is the flux at T_t after the end of the previous cycle, and D the polar flux at T_t after sunspot maximum. The shape of DE is only poorly known from observation.

To estimate the flux magnitude we assume that, in the absence of meridional motion, a one-dimensional random walk in the north-south direction would yield the distribution of flux in latitude. The fraction to be found at time τ between distances x and $x+dx$ from the point of release is then

$$W(x, \tau) dx = \frac{1}{2}(\pi D\tau)^{-\frac{1}{2}} \exp(-x^2/4D\tau) dx;$$

here a flux tube is supposed to make n_w displacements of length l_w positive or negative at random, in unit time, while $D = \frac{1}{2}n_w l_w^2$. For a supergranule with semi-diameter

$r = 15$ Mm, which breaks down after a day, then $n_w = 1$ and l_w has an average value of $2r/\pi$, about 9.5 Mm or 0.777° latitude. Hence D is about 0.302 (deg.)² per day. The fraction of the flux lying beyond x is $\int_x^\infty W(x, \tau) dx$, which tends to 0.5 as time increases indefinitely.

The meridional drift carries the centre of the distribution polewards, reducing the fraction of the flux lying beyond the equator at any one time to below that which would be present if there had been no drift. The approximate fraction lying across the equator at τ is obtained by taking x as the latitude ϕ_τ of the centre of the distribution at that time. Meridional motion in the opposite hemisphere takes flux there away from its point of origin. A good estimate of the fraction which has migrated permanently into the other hemisphere is given by the maximum W_{\max} of the integral $\int_x^\infty W(x, \tau) dx$ as τ increases.

We suppose that the poleward velocity takes the form $V_p = \alpha\phi^2$ in the latitude range $\phi \leq 10^\circ$. The value $V_p = 20 \text{ ms}^{-1}$ at $\phi = 10^\circ$ leads to the value $\alpha = 0.2 \text{ m s}^{-1}(\text{deg.})^{-2}$. Integrating we get

$$\tau = \alpha^{-1}(\phi_0^{-1} - \phi_\tau^{-1}),$$

where ϕ_0 is the latitude of the point of initial flux release, so that W_{\max} takes on the following values:

ϕ_0 (deg.)	10	8	6	4	2
W_{\max}	0.000	0.002	0.032	0.157	0.361

The rate of flux release as a function of latitude throughout the cycle is extremely difficult to extract from published data. The best approach seems to be the use of the sunspot area distribution and the inclination of spot-group axes, for both of which the resolution in latitude is poor. Antalova and Gnevyshev (1965) have plotted the average area distribution at 5° intervals of latitude through the cycle, from which 0.048 of the integrated sunspot area occurs at 5° , and 0.24 at 10° . We assume that flux released is proportional to sunspot area.

In general, the separation in longitude of the two main spots of a group exceeds 10° . Consequently, we again adopt 10° , whence the mean difference in latitude of follower and leader spots for a group centred on 5° is 0.63° , and the difference in the values of W_{\max} for the two spots averages 0.039. Of the total flux of each polarity released in a hemisphere, the net loss due to permanent migration across the equator is a factor of 0.048, representing a difference of 0.0019. A similar amount of the opposite polarity is gained from flux originating in the other hemisphere and crossing into the first, making the fraction 0.0038. Crude as the calculations and data are, this is about 0.5 of the flux which we have estimated to arrive in polar regions by the time ΔT_t after sunspot maximum. By these crude figures, the polar flux change from beginning to end of the cycle is about 0.4% of that of either polarity released during the cycle. This value is of similar magnitude to Babcock's (1961) crude estimate of the observed value of this fraction of 1%. A more detailed analysis based on data of higher resolution in latitude, and taking account of the flux contained in spot groups rather than mean areas, is much to be desired.

In the meantime, we can recognize the migration of net flux across the equator from low-latitude spot groups as the basic cause of cyclic polarity reversal in the polar field. A schematic diagram of the effect is given in Figs 2*c* and 2*d*, where the maximum flux at the end of the cycle is unknown and must be supplied by observation. But although observations cover about 25 years, they are far from homogeneous and it is difficult to sort out a good representative curve of polar field variation throughout the cycle. Field reversal occurs early in the cycle, apparently not later than sunspot maximum, although it may differ by up to two years in northern and southern hemispheres. The location of the polar field maximum and the shape of the curve from then until the end of the cycle are only vaguely known.

A consequence of the diffusion of predominantly leader flux across the equator in later stages of the cycle is a coupling between northern and southern hemispheres which, over a sufficient length of time, ensures the approximate equality of phases in field and cycle phenomena.

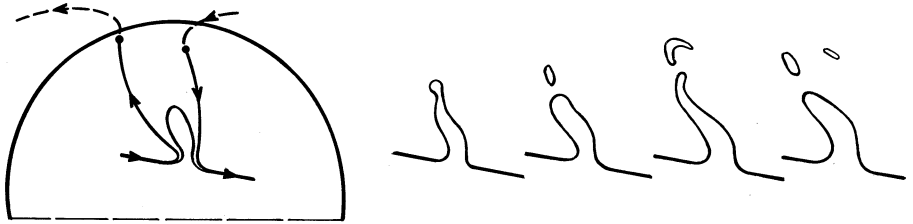


Fig. 3. Stages in loop formation, where loops formed by reconnection (as in Fig. 1*a*) are drawn polewards and eastwards by the poleward flow and differential rotation. The various gas motions result in the crossing of strands and further reconnection, and in the production of continuous loops which are annihilated during concentration processes when dragged into the slow equatorward flow.

6. Behaviour of Subsurface Flux Strands

(a) Strands Relating to Polar Regions

The reconnection of flux strands as in Fig. 1*a* produces submerged loops whose ends remain joined to the deep flux ropes from which the original strands were released. As the loops are drawn out in the poleward flow, further interaction between strands results in closed and submerged loops at the higher latitudes, such as shown in Fig. 3. Thus, in a simplified scheme, four sets of flux strands occur in the upper convection zone: (i) strands which have not taken part in reconnection processes; (ii) loops which, together with set (i), remain connected to the flux ropes in sunspot zones; (iii) submerged loops cut off from set (ii), in increasing numbers toward higher latitudes; and (iv) U-shaped loops complementary to set (ii), both ends passing through the surface. The U-shaped strands float eventually out of the Sun, either directly or after further reconnections which leave more cut-off loops. The absolute flux at the surface is thereby reduced; the additional cut-off loops so produced can be considered as additions to set (iii). There will also be variants on these basic sets.

We may note that continuous or ring-like cut-off loops from sets (ii) and (iii) make no contribution to the net fluxes involved. Despite their great numbers, they may be disregarded at this stage.

The surviving sets of strands (i), (ii) and (iii) are transported and distorted by convective or turbulent gas motions. As a result, individual strands will be dragged across one another, with frequent reconnections. On reaching polar regions, the counterflow carries these strands deep into the convection zone and back towards the equator. (The transport mechanism is described in detail in Part II.)

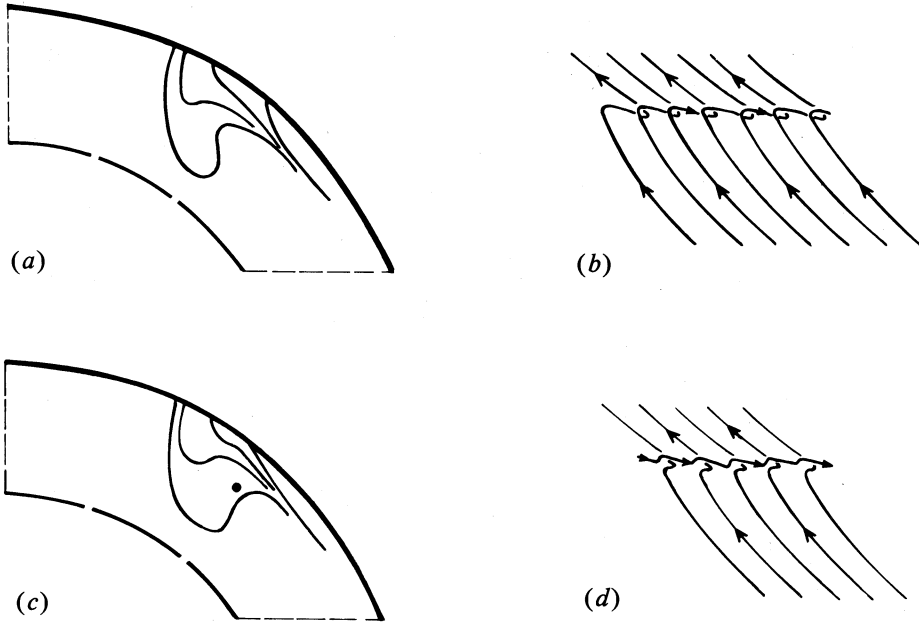


Fig. 4. (a) Successive appearances of flux strands carried to polar regions, as seen in latitude alone. The individual strands are inclined to the meridian because of differential rotation. (b) View of flux strands projected onto the disc. (c) The same strands after reconnection, shortening the extent of the upper bends, and producing an annular loop (marked by the dot) whose direction is opposite to those of the deeper strands; meridional section. (d) Projection of reconnected strands onto the disc. (Diagrams are not to scale.)

Strands of set (i) are shown in Fig. 4*a* in a highly simplified form projected onto a meridional plane; the corresponding disc projection is given in Fig. 4*b*. Convective motions up or down may conceivably drag parts of the bends of Fig. 4*a* into contact, in which case reconnection occurs. Since the strands are bent in three dimensions, two independent lines of force are connected in the process, leaving a shorter upper or lower bend together with, in the idealistic symmetrical case, an annular strand.

Very different consequences follow depending on whether the upper or lower bends of Fig. 4*c* are involved. If reconnection occurs mainly across the lower bends, negligible flux enters the equatorward stream, and the winding of flux ropes leading to sunspot formation cannot occur (such rope formation is impossible in the poleward stream because of the short time available). Neither is there any possibility of explaining the torsional oscillation. Both of these phenomena follow naturally if the reconnections are mainly in the upper bends.

There is also a more powerful argument. Reconnection across the lower bend merely restores the tube to its former configuration, whereas reconnection across the

upper bend leads to permanent and irreversible changes. Therefore, it is inevitable that, over a period of time, this process must predominate.

On average, the annular strands produced in the process lie ultimately in the upper part of the equatorward flow. They undergo no shear or concentration because, on average, they are concentric with the rotation axis. However, they will reconnect frequently, mainly with the inflection regions of the bends. Such interactions would seem to have little effect on the overall behaviour. The final effect is as if the strands from polar regions were dragged down into the equatorward stream at ever-decreasing latitudes. There the strands undergo winding, shearing and concentration, and convective and turbulent motions drag the strands together. Where they cross at appreciable angles, reconnection takes place as described in Section 2 and shown in Fig. 1*a*.

At times, the angle between the axes of flux tubes may be very small (see Fig. 1*b*). In Part II we show how such tubes can be dragged or twisted into contact. The rate at which gas and field can be withdrawn from a point of contact then becomes very small, since only a very small component of the magnetic tension can act in the withdrawal direction. Thus, reconnection becomes very slow; the very gentle twists survive to give rise to the twisted flux ropes required by Piddington to explain the surface phenomena and to prevent dispersal of the ropes.

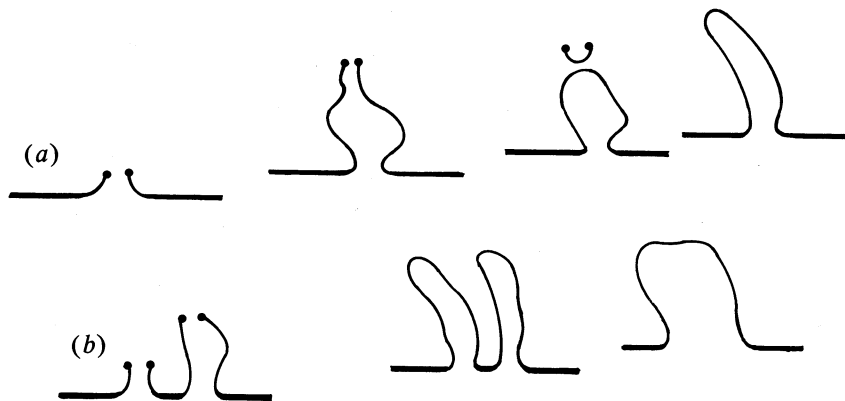


Fig. 5. Disc projection of representative strands involved in subsurface flux-loop production after dispersal from sunspots: (a) single flux loop and (b) pair of flux loops from neighbouring spot groups later in the cycle. Floating of the flux rope between the two groups reduces the loops from two to one.



Fig. 6. Disc projections of flux strands at various stages in the dispersal of a segment of flux rope near the end of a cycle. The last spot group produced by the segment erupts in the middle diagram.

Floating of these ropes, studied in detail in Part II, gives rise to sunspot formation when they intersect the surface. Spruit (1977) has shown how this results in a reduction in the rate of convective heat transfer and consequently a dark spot where the field is strong. The subsequent sequence of events has been summarized by Piddington (1976*a*).

(b) Loops of Set (ii) Late in the Cycle

Early in the cycle, the flux from the ropes which have produced sunspots goes mainly into flux loops of set (ii), with a small fraction involved in set (i). Later in the cycle, the rate of sunspot production falls, and loop production ceases when sunspots no longer appear. Fig. 5 shows how this occurs. In (a), representative strands disperse from a pair of sunspots, the subsurface rope being shown by the heavy line. The subsequent views show the formation of the subsurface loop. Later in the cycle, when short lengths of rope between groups float to the surface, the number of loops is reduced (see Fig. 5*b*). The floating of flux ropes also involves reconnection with surviving annular flux strands. The resulting tube configurations are quite varied, and no attempt is made to describe them here.

At the end of the cycle, the last remaining segments of flux ropes are heavily frayed at the ends, as shown in Fig. 6. On the formation of the last group from a segment, the flux strands are swept polewards by the meridional flow except for those, predominantly of leader polarity, which diffuse across the equator. The concentration of subsurface loops is maximum when about one-half of the total flux for the cycle has erupted, on average about a year after sunspot maximum.

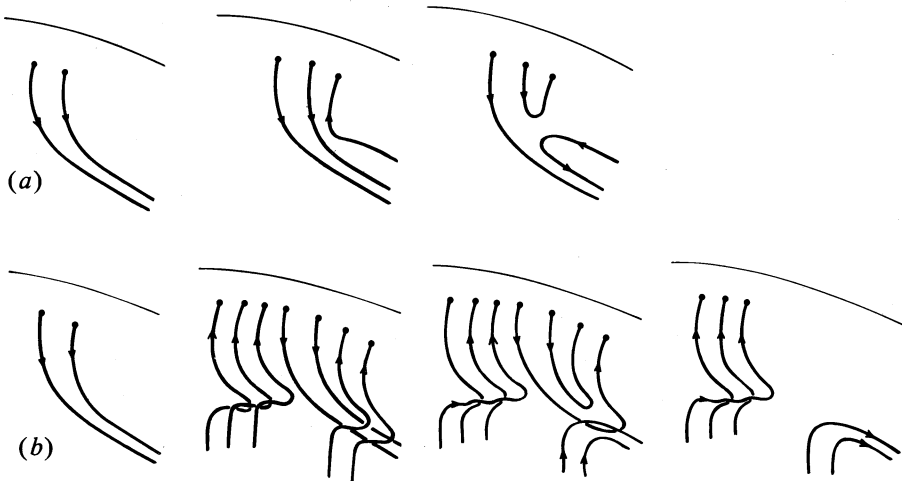


Fig. 7. Consecutive stages in the reversal of polar field: (a) Meridional view, showing the effect of a strand of opposite polarity arriving in polar regions. The U-shaped loop floats off eventually, perhaps after further reconnections. (b) Projection onto the disc at successive stages after the arrival of several strands of opposite polarity.

(c) Behaviour of Flux Strands Near Polar Field Reversal

The behaviour of flux strands and ropes near the time of the polar field reversal is illustrated in Fig. 7*a*, which shows in meridional projection the arrival of a strand of reverse polarity reconnecting to one of the old strands and reducing the surface

flux when the upper U-shaped loop floats off. Fig. 7*b* is a time sequence showing, projected onto the disc, the arrival of reverse flux strands which, in part, reconnect to the weakened flux rope as in Fig. 7*a*. They represent the end of the old cycle fields. The other strands of Fig. 7*b* reverse the polar field and give rise to the beginning of a new flux rope of reverse polarity and to the partial development of an annular-shaped strand around a parallel of latitude.

Throughout the cycle, deep flux ropes develop as the concentration of sheared flux strands increases. Random events lead to non-uniformities in the distribution of flux strands. In close analogy with Babcock's (1961) description, this leads to the production of more-or-less separate concentrations of flux ropes whose cross sections will vary along their lengths.

(d) Concentration of Flux Strands in Equatorward Flow

We now discuss the way in which differential rotation concentrates flux tubes in the equatorward flow, using the following simplifications: (i) flux tubes lie along stream lines; (ii) the mean 'polar' field strength at latitude ϕ_p varies with time according to a simple arbitrary model; (iii) flux strands which do not intersect the surface can be disregarded; (iv) the velocity of the equatorward flow is given; and (v) angular rotation takes the form

$$\omega = \Omega - b \sin^2 \phi - c \sin^4 \phi \tag{6}$$

where, from Howard (1978),

$$\Omega = 2.78 \mu\text{rad s}^{-1}, \quad b = 0.352 \mu\text{rad s}^{-1}, \quad c = 0.442 \mu\text{rad s}^{-1}.$$

In the time t , the decrease in latitude ϕ of a gas sample due to the equatorward flow is

$$\phi_p - \phi = \int_0^t \frac{V^*}{R_\odot} dt = \frac{V^*}{R_\odot} t,$$

where the gas starts from latitude ϕ_p at time zero, and in the first instance the velocity V^* is taken to be constant.

The angle through which the gas rotates about the solar axis, with respect to its place of origin, is

$$\begin{aligned} \theta &= \int_0^t (\Omega - b \sin^2 \phi - c \sin^4 \phi) dt - \int_0^t (\Omega - b \sin^2 \phi_p - c \sin^4 \phi_p) dt \\ &= (R_\odot / V^*) \int_{\phi_p}^{\phi} (b \sin^2 \phi + c \sin^4 \phi) d\phi + (b \sin^2 \phi_p + c \sin^4 \phi_p) t \\ &= (R_\odot / V^*) [(\phi - \phi_p) \{ \frac{1}{2}(b + c) \cos 2\phi_p - \frac{1}{8}c \cos 4\phi_p \} - \frac{1}{4}(b + c)(\sin 2\phi - \sin 2\phi_p) \\ &\quad + \frac{1}{32}c(\sin 4\phi - \sin 4\phi_p)]. \end{aligned}$$

The angle to the meridian made by a line of force following the gas motion is given by

$$\tan \psi = \frac{d\theta}{d\phi} = \left(\frac{R_{\odot}}{V^*} \right) \left\{ \frac{1}{2}(b+c)(\cos 2\phi_p - \cos 2\phi) - \frac{1}{8}c(\cos 4\phi_p - \cos 4\phi) \right\}. \quad (7)$$

Then the flux is concentrated by a factor

$$\mathcal{G} = (A_{\phi_p}/A_{\phi}) \sec \psi, \quad (8)$$

where A_{ϕ} is the cross sectional area of the equatorward flow at latitude ϕ . The concentration of flux tubes at ϕ and t has the value $\mathcal{G} m_0$, where m_0 is the concentration at ϕ_p at time $t = 0$. If V^* is non-uniform, it is simplest to use a similar procedure in steps, in each of which V^* is uniform.

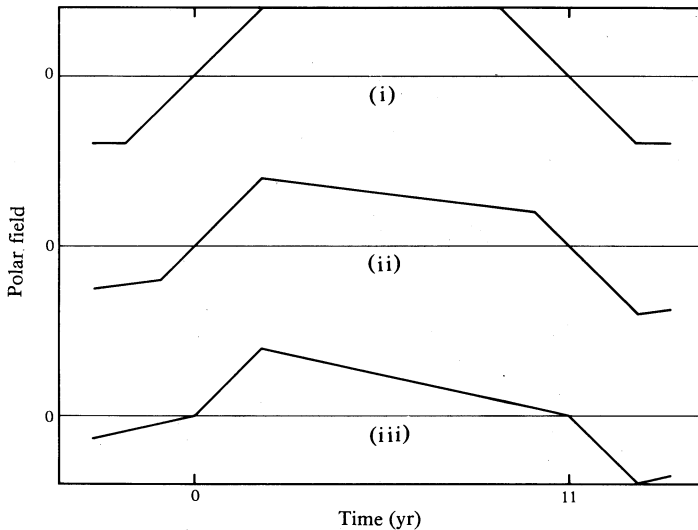


Fig. 8. Three models of the variation of polar field throughout the cycle: (i) a long time with uniform field, changing to opposite polarity at a uniform rate; (ii) uniform drop from field maximum to a value of one-half maximum at time T after the end of a sunspot cycle; and (iii) uniform drop in field from maximum to reversal.

We assume here that there is a one-to-one relation between the radius of the ropes produced and the concentration of flux tubes. The critical value of the latter for floating and producing sunspots is then given by its value on the outbreak of new cycle sunspots at $\phi = 30^\circ$. For assessing the course of the cycle, we have made calculations using three models of the mean polar field, as shown in Fig. 8. Rather than the values of V^* taken directly from Table 2, values have been chosen to fit the mean variation of sunspot latitude with time. But this yields V^* only for $\phi < 30^\circ$. For higher latitudes, we recall that reversal of polarities in polar regions follows some two or three years after outbreak of the sunspot cycle. The time lag is taken quite arbitrarily as two years, with the location of ϕ_p at 70° . This is achieved if the

equatorward flow moves from 70° to 30° latitude in seven years at a mean velocity of $5.7^\circ \text{ yr}^{-1}$. The increase in V^* over this range is assumed to be linear, starting from the value of $3.8^\circ \text{ yr}^{-1}$ found for the range 26.2° to 30° latitude. The empirical values are given in Table 3.

Table 3. Empirical values of V^*

Values of V^* are given in both units of deg. yr^{-1} and (in parentheses) ms^{-1}

ϕ (deg.)	V^*	ϕ (deg.)	V^*	ϕ (deg.)	V^*
7.4	0.7 (0.27)	15.7	3.1 (1.19)	39.2	5.2 (2.00)
8.1	1.0 (0.38)	18.8	3.7 (1.42)	44.4	5.8 (2.23)
9.1	1.1 (0.42)	22.5	3.7 (1.42)	50.2	6.1 (2.34)
10.2	1.4 (0.54)	26.2	3.8 (1.46)	56.3	6.7 (2.57)
11.6	1.8 (0.69)	30.0	4.3 (1.65)	63.0	7.0 (2.69)
13.4	2.3 (0.88)	34.3	4.9 (1.88)		

Comparison with Table 2 shows quite good agreement with the values for $ZP = 62.2 \text{ Mm}$ at $\phi = 10^\circ$. The only substantial differences are at very low and very high latitudes (10° and 70°). At low latitudes V^* falls off towards zero near the equator as required. Nevertheless, the base of the region of poleward flow must be somewhat deeper than 62.2 Mm , as $\bar{V}_p = 20 \text{ ms}^{-1}$ was assumed for the values in Table 2. This is probably an overestimate by an unknown amount, but the base should not be too much deeper than 62.2 Mm . Because of this, the cross sectional area of the counterflow may not vary too greatly, and we have simplified the calculations by taking A_ϕ independent of latitude. This may introduce small changes in flux concentration at higher latitudes, but there is no error in the relative time variation at a given latitude, nor any significant change in sunspot latitudes. How can we provide an empirical description agreeing with these requirements?

Fig. 9 plots the sunspot curves for the three types of polar field, based on the location in time of the critical value of the calculated flux concentration at a given latitude; this is taken as the maximum value reached at 30° . At lower latitudes, there is a range of time during which the concentration exceeds this minimum, although the ranges shown are too extensive because no allowance has been made for losses due to sunspot production; the cycle dies out when the flux ropes have all floated upwards, leaving no remainder for further concentration.

The three types of polar field have identical onsets, and the maxima of types (ii) and (iii) are identical. Type (i) has an extended maximum whose beginning coincides with the other two maxima. The durations of the sunspot curves drop off from types (i) to (iii). The curve giving the maximum rate of sunspot production in types (ii) and (iii), and the onset of maximum in type (i), agrees with the mean observed sunspot curve (because it was designed to do so).

The calculated reversal of the polar field (at 70°) occurs two years after outbreak of the sunspot cycle, as planned. The period of the full magnetic cycle is twice that of two individual sunspot cycles. Each of these occupies the two-year delay from the outbreak of a cycle to the polar field reversal (including the one-year transit time of flux from 30° to 70°), the two years adopted from then until polar field maximum, and seven years in drifting down to 30° in the equatorward flow, making 11 years in all. This period is dictated mainly by the meridional circulation velocities. Their

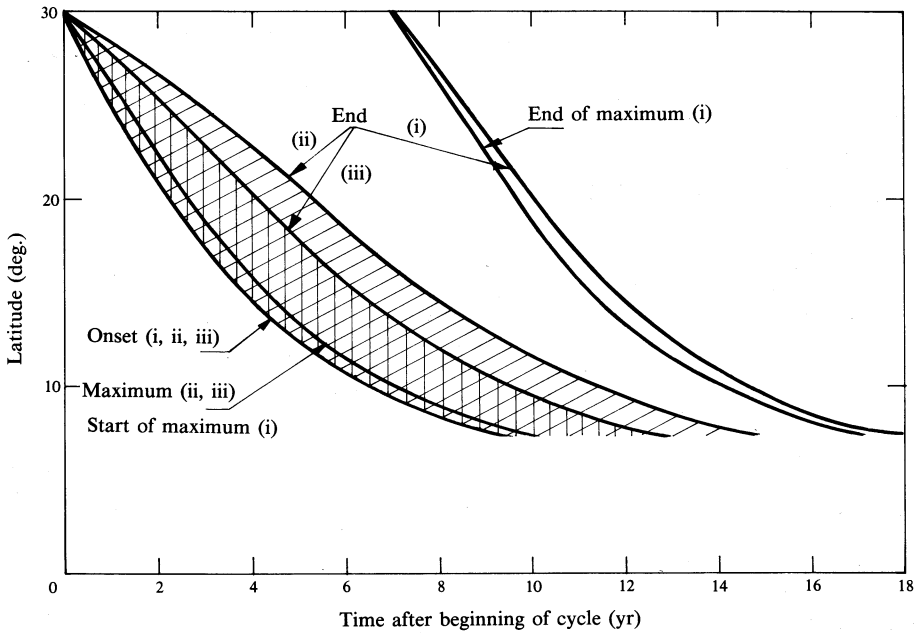


Fig. 9. Final calculated curves for the variation of sunspot production with latitude and time for polar fields of types (i), (ii) and (iii) (see Fig. 8). The onset and end are shown for each, the areas being hatched for types (ii) and (iii). For all types the onsets are identical, as are the curves of maximum sunspot production in types (ii) and (iii) and the onset of the extended maximum in type (i). The durations are too long as they make no provision for the loss of flux by sunspot production. In practice, the edges of the sunspot zones would be diffuse.

order of magnitude has been calculated from the observed surface poleward flow, and they have then been adjusted empirically to fit the observed cycle phenomena. The Hale and the Spörer laws follow automatically.

7. Torsional Oscillations and Their Phase Relationships

The field concentration is increased by differential rotation, and the field reacts so as to reduce the differential rotation. This produces a departure Δ from the average rate of rotation ω , where $|\Delta| \ll \omega$. Since $\partial\omega/\partial\phi$ is negative, the reaction *increases* $\omega + \Delta$ as a function of ϕ ; this may be expressed as

$$\frac{\partial^2}{\partial t^2} \left(\frac{\partial(\omega + \Delta)}{\partial \phi} \right) \equiv \frac{\partial^2}{\partial t^2} \frac{\partial \Delta}{\partial \phi} = k|B|, \quad (9)$$

since the reaction is independent of the sign of B , k being a positive constant.

Two possible field structures may contribute significantly to (9), the ropes in the equatorward flow, and the cut-off loops of set (iii). The effects of tubes which lie in the upper convection zone are negligible; the U-shaped strands of set (iv), which float out from the Sun, are very weak by comparison with set (ii), which in turn make little

contribution because of the small shearing during transit in the poleward stream. The annular rings of Fig. 4 are not sheared and make no contribution.

In the Appendix we show that, for the ropes in the equatorward flow, each harmonic i of $|B|$ at a given latitude produces a corresponding harmonic of Δ leading it by time $T_c/4i$, where T_c is the length of the sunspot cycle and i is the number of the harmonic. Since the strongest harmonics of the absolute polar flux have $i = 1$ or 2, then the maximum in Δ occurs about $T_c/4$ to $T_c/8$ before the maximum in $|B|$. Thus, in sunspot zones, the maximum of Δ occurs some 1.5 to 3 years before maximum sunspot activity at the same latitude. The approximate locations predicted for maximum Δ are compared with the LaBonte and Howard (1982) observations in Fig. 10, the curves being superimposed at latitude 30° . Below 15° and above 55° the LaBonte–Howard data involve different cycles, whose phasing is somewhat uncertain with respect to the middle range. However, agreement is very good for latitudes below 50 – 55° with respect to both the variation of phase with time and its relation to the sunspot curve. There appears to be a shift in phase (but not in gradient) of about four years at latitudes near 55° for the first few years after reversal of the polar field. Whether or not such behaviour is systematic will require further observations to establish.

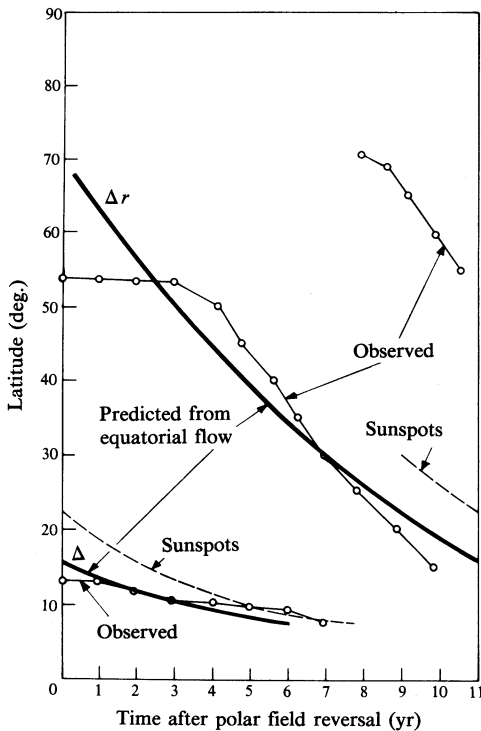


Fig. 10. Comparison of predicted phase of the torsional oscillation (maximum variation in Δ from mean rotational velocity at latitude ϕ) with the LaBonte and Howard (1982) oscillation observations and maximum sunspot activity, when averaged over northern and southern hemispheres.

Until annihilated, the continuous cut-off loops of set (iii) have effects rather like those of the strands or ropes of the equatorward flow. Although their numbers may be much greater initially, individual loops are unlikely to react on differential rotation as strongly as the strands or ropes since the loops are free during extension. We have little way of ascertaining how important they are to the torsional oscillation.

8. Review and Comments

We have described how surface observations of motions and magnetic fields combine to provide a fairly unique model of the sunspot and magnetic cycle phenomena. Flux released from sunspots is dispersed by supergranule motions, and carried polewards by a meridional flow of $\sim 20 \text{ m s}^{-1}$. Because of the tilt of spot-group axes, flux from follower spots arrives in polar zones two weeks or so before leader flux until sunspot maximum. This results in the arrival of more follower than leader flux and the consequent reversal of the polar field. Later in the cycle, when some sunspots appear close to the equator, flux can be dispersed into the other hemisphere by supergranule motions, more from the leader than the follower. Calculations show that this plus the complementary flow of flux from the opposite hemisphere is of the correct magnitude to account for the observed net change in polar flux during the cycle.

The processes described above involve much reconnection of magnetic flux tubes. This takes place readily wherever tubes are dragged into contact at appreciable angles.

Just as flux tubes are transported polewards by the slow drift velocity, so they must be carried downwards at high latitudes and then even more slowly equatorwards deep in the convection zone. The physics of the interactions between the flux tubes and surrounding medium is investigated in Part II.

Deep in the convection zone, the concentration of flux tubes by differential rotation gives rise to the formation of flux ropes which are twisted very gently and undergo reconnection only very slowly. Details of rope formation and of floating when the ropes are large enough are also given in Part II.

Winding of the flux tubes by differential rotation results in a reaction which tends to reduce differential rotation. It is shown that this varies the phase of solar rotation in the way observed in the torsional oscillation (LaBonte and Howard 1982). The amplitude of the oscillation is also among the subjects deferred until Part II.

Overall a satisfying account emerges of the main cycle phenomena. These turn out to be self-consistent and in agreement with surface observations. As shown in Part II, the results are in major disagreement with all previous attempts to account for the cycle, the differences being traced to fundamental errors and omissions in the physics of those earlier analyses.

References

- Antalova, A., and Gnevyshev, M. N. (1965). *Sov. Astron.* **9**, 198.
 Babcock, H. W. (1961). *Astrophys. J.* **133**, 572.
 Brunner, W. (1930). *Astron. Mitt. Zürich* **124**, 67.
 Cowling, T. G. (1981). *Annu. Rev. Astron. Astrophys.* **19**, 115.
 Duvall, T. L. (1979). *Sol. Phys.* **63**, 3.
 Giovanelli, R. G. (1977). *Sol. Phys.* **52**, 315.
 Giovanelli, R. G. (1982). *Sol. Phys.* **77**, 27.
 Giovanelli, R. G. (1985). *Aust. J. Phys.* **38**, 1067.
 Harvey, J. W. (1977). In 'Highlights of Astronomy', Vol. 4, Part II (Ed. E. A. Müller), p. 223 (Reidel: Dordrecht).
 Howard, R. (1974). *Sol. Phys.* **38**, 59.
 Howard, R. (1978). *Rev. Geophys. Space Phys.* **16**, 721.
 Howard, R., and LaBonte, B. J. (1980). *Astrophys. J.* **239**, L33.
 Howard, R., and LaBonte, B. J. (1981). *Sol. Phys.* **74**, 131.
 LaBonte, B. J., and Howard, R. (1982). *Sol. Phys.* **75**, 161.
 Leighton, R. B. (1964). *Astrophys. J.* **140**, 1547.
 Livingston, W., and Harvey, J. W. (1975). *Bull. Am. Astron. Soc.* **7**, 346.

- Petschek, H. E. (1964). *Symp. on the Physics of Solar Flares* (Ed. W. N. Haas), p. 425 (NASA: Washington, D.C.).
- Piddington, J. H. (1975). *Aust. J. Phys.* **32**, 671.
- Piddington, J. H. (1976a). In 'Basic Mechanisms of Solar Activity', IAU Symp. No. 71 (Eds V. Bumba and J. Kleczek), p. 389 (Reidel: Dordrecht).
- Piddington, J. H. (1976b). *Astrophys. Space Sci.* **45**, 47.
- Piddington, J. H. (1979). *Astrophys. J.* **233**, 727.
- Piddington, J. H. (1981). *Astrophys. Space Sci.* **75**, 273.
- Priest, E. R., and Soward, A. M. (1976). In 'Basic Mechanisms of Solar Activity', IAU Symp. No. 71 (Eds V. Bumba and J. Kleczek), p. 353 (Reidel: Dordrecht).
- Richardson, R. S., and Schwarzschild, M. (1953). *Accad. Lincei Convegno Volta* **11**, 228.
- Spörer, G. (1894). *Publ. Potsdam Obs.* **10**, 144.
- Spruit, H. C. (1974). *Sol. Phys.* **34**, 227.
- Spruit, H. C. (1977). *Sol. Phys.* **55**, 3.
- Stenflo, J. O. (1976). In 'Basic Mechanisms of Solar Activity', IAU Symp. No. 71 (Eds V. Bumba and J. Kleczek), p. 69 (Reidel: Dordrecht).
- Tuominen, J. (1941). *Z. Astrophys.* **21**, 96.
- Tuominen, J. (1976). *Sol. Phys.* **47**, 541.

Appendix: Torsional Oscillations

We consider here the ropes in the equatorward flow and expand $|B|$ in harmonics:

$$|B| = \sum_i \sum_j B_{ij} \sin(Y_{ij} + \alpha_{ij}) + B_m,$$

where

$$Y_{ij} = 2i\pi t/T_c + 4j\phi,$$

T_c is the length of the sunspot cycle, the α_{ij} are constants, the B_{ij} are positive and B_m is the mean value of the field over the cycle.

We seek a solution to (9) of the form

$$\Delta = \sum_i \sum_j A_{ij} \sin(Y_{ij} + \epsilon_{ij}),$$

where the ϵ_{ij} are constants and the A_{ij} are positive. Then we have

$$\begin{aligned} \frac{\partial^2}{\partial t^2} \frac{\partial \Delta}{\partial \phi} &= \frac{16\pi^2}{T^2} \sum_i \sum_j i^2 j A_{ij} \cos(Y_{ij} + \epsilon_{ij}) \\ &= k \left(\sum_i \sum_j B_{ij} \sin(Y_{ij} + \alpha_{ij}) + B_m \right). \end{aligned}$$

For this relation to hold, we require

$$-\cos(Y_{ij} + \epsilon_{ij}) = \sin(Y_{ij} + \alpha_{ij}).$$

whence

$$\epsilon_{ij} = \frac{1}{2}\pi + \alpha_{ij}.$$

Then we get

$$Y_{ij} + \epsilon_{ij} = 2i\pi t/T_c + 4j\phi + \alpha_{ij} + \frac{1}{2}\pi.$$

Thus, each harmonic of Δ has a maximum at time $T_c/4i$ before the maximum of the corresponding harmonic of $|B|$.

Manuscript received 9 May, accepted 23 July 1985